

Nanocrystalline CdSe Formation by Direct Reaction between Cd Ions and Selenosulfate Solution

Shira Yochelis and Gary Hodes*

Department of Materials and Interfaces, Weizmann Institute of Science, Rehovot 76100, Israel

Received January 18, 2004. Revised Manuscript Received March 2, 2004

We investigate the reaction between selenosulfate and (noncomplexed) Cd ions in aqueous solution to form CdSe. The resulting precipitate, which is initially white (mainly CdSO_3), turns yellow and finally orange. The initial precipitate is CdSO_3 , which gradually reacts with selenosulfate to give CdSe. The CdSe forms as a disordered phase surrounding the CdSO_3 , and this largely amorphous CdSe breaks off from the CdSO_3 crystals to form nanocrystals of CdSe. The color changes during the reaction, due to size quantization of the CdSe nanocrystals, were correlated with the measured CdSe crystal sizes.

Introduction

The reaction between selenosulfate and Cd ions is the basis of the most commonly used technique for chemical bath deposition (CBD) of CdSe films.¹ These films are composed of nanocrystals of CdSe, with sizes ranging between 3 and 20 nm, depending on deposition conditions, and the smaller ones show clear spectral blue shifts due to size quantization.² Despite the considerable amount of work on this system, the exact mechanism of the reaction is not known with certainty. It has been clearly demonstrated that the reaction can proceed either through a solid hydroxide phase, which is converted to CdSe, or by a direct reaction involving Cd^{2+} ions.³ However, whether this reaction involves free (hydro)selenide ions or some complex between the selenosulfate and the Cd species is still an open question (and one which we are presently investigating).

The Cd is normally complexed in the CBD process to prevent (gross) $\text{Cd}(\text{OH})_2$ precipitation at the relatively high pH values normally used, as well as to control the rate of the overall reaction; in the absence of a complexant for Cd, a precipitate is rapidly formed and little or no film formation occurs. This complex-free reaction has been used in very few studies: PbSe precipitate⁴ and more recently CdSe colloidal quantum dots⁵ have been obtained in this manner.

In this paper, we study this (complex-free) precipitation, following the gradual transformation of initially precipitated CdSO_3 to CdSe by transmission electron microscopy/electron diffraction, X-ray diffraction, and optical spectroscopy, the last providing a measure of CdSe crystal size through size quantization. Such a study may also help in better understanding some aspects of the mechanism of formation of CdSe in CBD.

Experimental Section

Sample Preparation. Four milliliters of aqueous sodium selenosulfate (Na_2SeSO_3 , 0.2 M Se dissolved in 0.5 M Na_2SO_3) was added in a single step to 6 mL of a 0.095 M aqueous solution of CdSO_4 (final concentrations: 57 mM CdSO_4 , 80 mM selenosulfate) at room temperature (the pH of the final solution is between 7 and 8). A nominal excess (1.4 times) of selenosulfate is used both to compensate for the fact that not all the 0.2 M Se dissolves in the sulfite and also because elemental analysis (microprobe) showed that, with less selenosulfate, the final precipitate contains fairly large amounts of slightly soluble CdSO_3 since there is not enough active Se to react with all the Cd ions.

Characterization Methods. *Transmission Electron Microscopy/Electron Diffraction (TEM/ED).* A Philips CM120 electron microscope operating at 120 kV was used for transmission electron microscopy and electron diffraction in the selected area mode. Samples were dried onto carbon-coated copper grids (400 mesh). To measure size distributions of crystals which were irregularly shaped (most were fair approximations of a sphere), the crystal was treated as a sphere with a radius the sum that of the large axis + twice the short axis and divided by three.

X-ray Powder Diffraction (XRD). Powder X-ray diffraction (XRD) spectra of powders dried on a glass substrate were recorded on a Rigaku RU-200B Rotaflex diffractometer operating in the Bragg configuration using $\text{Cu K}\alpha$ radiation. The accelerating voltage was set at 50 kV with a current of 150 mA. Scatter and diffraction slits of 1° and a 5-mm collection slit were used. Coherence length (assumed equal to crystal size) was estimated using the Scherrer equation based on XRD peak broadening.

Optical Spectroscopy. The optical transmittance spectra of CdSe in solution were recorded using a JASCO V-500 UV/VIS spectrophotometer, fitted with an integrating sphere, in the 400–700 nm range.

Elemental Analyses. (1) *Scanning Electron Microscopy/Energy Dispersive Spectrometry (SEM/EDS).* A JEOL, JSM-6400 microscope operating at 15 kV, WD = 15 mm, was used for EDS analyses. Samples were taped to carbon and then carbon-coated.

(2) *Inductively-Coupled Plasma Optical Emission Spectroscopy (ICP-OES).* A Spectroflame ICP-OES modular E. system was used. Samples were rinsed three times with doubly distilled water (DDW) and then dissolved in concentrated HNO_3 and diluted by 10000 times with DDW.

(1) Hodes, G. *Chemical Solution Deposition of Semiconductor Films*; Marcel Dekker: New York, 2002.

(2) Hodes, G.; Albu-Yaron, A.; Decker, F.; Motisuke, P. *Phys. Rev. B* **1987**, *36*, 4215.

(3) Gorer, S.; Hodes, G. *J. Phys. Chem.* **1994**, *98*, 5338.

(4) Glistenko, N. E.; Yermmina, A. A. *Zh. Neorg. Khim.* **1960**, *5*, 1003.

(5) Xu, L.; Chen, K.; Zhu, J.; Chen, H.; Huang, H.; Xu, J.; Huang, X. *Superlattices Microstruct.* **2001**, *29*, 67.

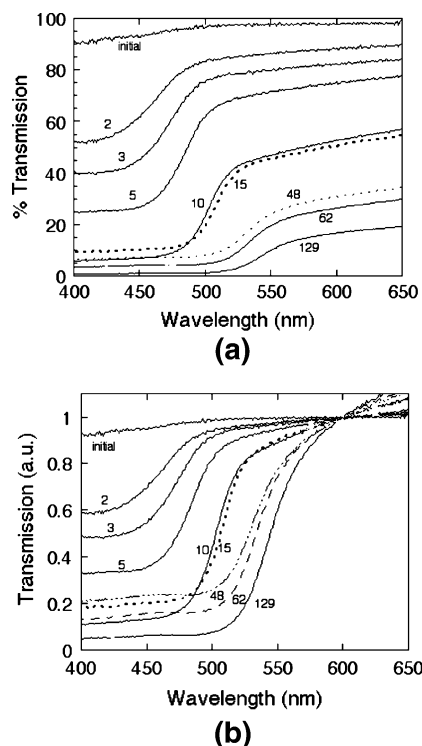


Figure 1. (a) Evolution of the transmission spectra of $\text{CdSO}_4/\text{Na}_2\text{SeSO}_3/\text{Na}_2\text{SO}_3$ reactant mixture with time. Aliquots were diluted three times with water immediately before each measurement. (b) Like (a), but normalized at 600 nm with a normalized transmission axis.

Results and Discussion

The initially formed suspension is white and turns yellow within a few minutes, at the same time gradually precipitating. The suspension and precipitate continue to change color, eventually becoming orange. These color changes are shown in the transmission spectra of Figure 1a,b. There is a gradual red shift of the absorption onset as the reaction proceeds, together with decreasing transmission due to flocculation and subsequent light scattering by the product (this occurs even using the integrating sphere since a large part of the scattered light can be lost before entering the sphere). Since the initial color change is rapid, we also carried out a similar kinetic study, only using a much more dilute solution (by 30 times) in order to better see the initial progression. This also reduces the scattering loss. Figure 2a shows the spectral changes while the same set of spectra is shown at higher transmission sensitivity in Figure 2b to show more clearly the change in absorption onset. The gradual red shift with progressing reaction is seen more distinctly. In addition, there is a small red shift of ca. 10 nm in the spectra (initial and final) of the diluted solution compared to the original one. The slight red shift in the spectra of the dilute solutions (Figure 2) compared to more concentrated ones (Figure 1) noted previously can be explained by slower growth of thermodynamically unstable nuclei in more dilute solution and therefore a greater chance of these nuclei redissolving, resulting in a smaller number of nuclei which eventually grow into stable crystals. Since the final crystal size depends on the amount of reactant per stable nucleus, the result is a larger final crystal size (see p 348 of ref 1).

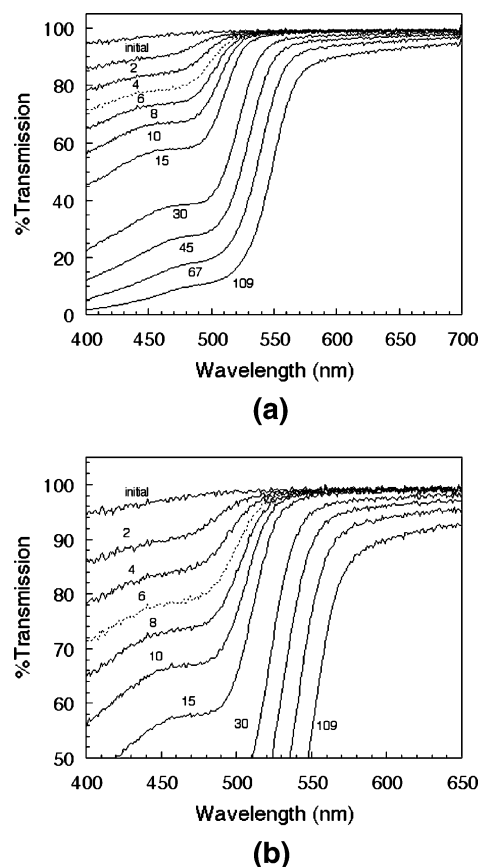


Figure 2. (a) Like Figure 1a, but reactant concentration 1/30 of that of Figure 1a. (b) Like Figure 2a with an expanded transmission axis.

Since the selenosulfate solution always contains an excess of sulfite, we first studied the precipitation of (what we presumed to be) CdSO_3 by adding Na_2SO_3 to a solution of CdSO_4 (at a final pH of ca. 7.5). The XRD spectrum of this precipitate is for the most part similar to PDF 31-0240, $2\text{CdSO}_3 \cdot 13\text{H}_2\text{O}$, although it is probable that other forms of CdSO_3 may also be present to some extent ($\text{Cd}(\text{OH})_2$ is not seen in XRD). This spectrum contains many peaks and they vary considerably in relative intensity from precipitation to precipitation as well as from measurement to measurement for the same sample.

Attempts to analyze the initial white suspension formed in the reaction between CdSO_4 and selenosulfate (even in a cooled solution) by XRD were unsuccessful since we were unable to filter or centrifuge it in the early stages of formation, and by the time we could, it had already turned yellow. We were able to freeze the white precipitate in liquid nitrogen and carry out a cryoTEM study. ED of these samples showed, among other reflections, three prominent ones at low angles (forming a fairly closely spaced triplet) characteristic of the CdSO_3 hydrate noted above as measured by XRD (PDF 31-0240).

A chemical consideration of the initial white precipitate suggests that it is mainly CdSO_3 (most likely since CdSO_3 is almost insoluble in water and there is an excess of sulfite ions), but it could in principle be a CdSeSO_3 species (although it should be noted that the analogous S compound, CdS_2O_3 , is soluble), and possibly some $\text{Cd}(\text{OH})_2$ which might also form at the pH used

(although precipitation of CdSO_3 at the same pH showed no evidence of $\text{Cd}(\text{OH})_2$ formation by XRD). Therefore, we can describe the first stage of the reaction by eq 1:



We next consider the yellow precipitate, which starts to form within a few minutes after the start of the reaction between CdSO_4 and selenosulfate. It should be noted that separation of the precipitate by centrifugation takes about 5 min from the start of the reaction and the reaction can continue during this process.

Both EDS and atomic absorption (ICP) methods were used to analyze the samples. Each method has limitations (e.g., matrix effects for EDS and loss of S (as SO_2) and Se (as H_2Se) on acidification for ICP).

EDS analyses showed that this precipitate contained nearly 3 times as much S as Se (molar ratios) and somewhat more Cd than the sum of the S and Se ($[\text{Se} + \text{S}]/\text{Cd} \approx 0.8$). ICP gave a S:Se ratio of 1.8 and $[\text{Se} + \text{S}]/\text{Cd} = 0.83$. In both cases, we can conclude that most of the Cd exists as CdSO_3 , with some CdSe and also a little $\text{Cd}(\text{OH})_2$ (the latter is the only expected species which would explain the excess Cd). We note that if the initial precipitate were indeed CdSeSO_3 , the Se:S ratio should be unity. Therefore, together with the anticipated solubility of such a compound, it is unlikely that the initial precipitate is CdSeSO_3 .

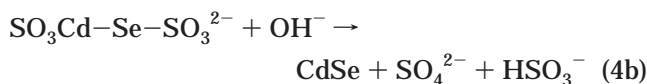
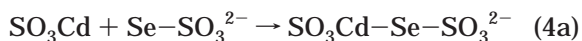
The two most likely pathways for formation of the CdSe are as follows: (a) hydrolysis of SeSO_3^{2-} to HSe^- . The overall equation for this reaction is generally given as



followed by



or (b) complex formation between SeSO_3^{2-} and CdSO_3 followed by decomposition of this complex:



(There will be various equilibria between HSe^- and Se^{2-} , HSO_3^- and SO_3^{2-} , and probable final formation of SO_4^{2-} . We do not attempt to differentiate between these various possibilities and intermediates).

A TEM study of the yellow precipitate shows that it is comprised mainly of crystals between 1.5 and 4.5 nm and with a small concentration of larger crystals: the average size is 3.1 nm (Figure 3). The lattice spacing of the large crystals are consistent with those of CdSO_3 or CdSe but not with $\text{Cd}(\text{OH})_2$. Those of the small crystals match hexagonal CdSe (lines characteristic of hexagonal CdSe —2.15, 3.29, and 2.55 Å—are seen, but this does not rule out the presence of cubic CdSe as well). Of particular note, the smaller crystals (believed to be CdSe) are separated from the larger ones (believed to be CdSO_3). However, a close look at a particularly large crystal (upper left in Figure 3) shows that it is surrounded by a disordered phase with a characteristic

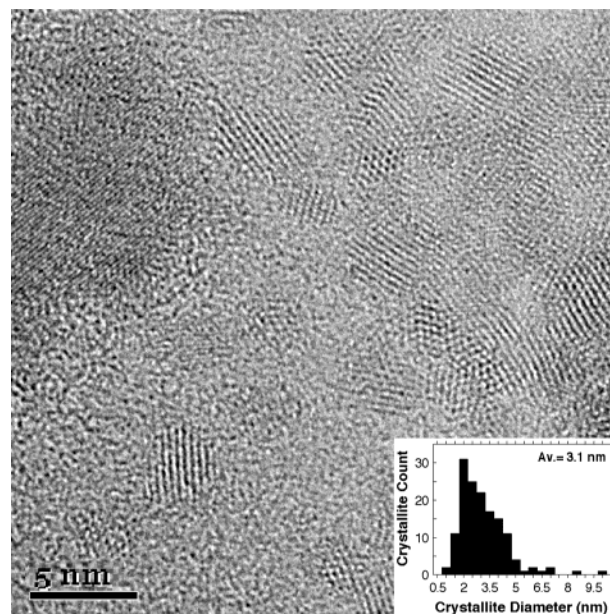


Figure 3. High-resolution TEM micrograph of the yellow precipitate. Inset: Size distribution of the crystals in this precipitate. Note that not all of these crystals are CdSe .

spacing similar to that of the CdSe crystals. This indicates that the mechanism of formation of CdSe is exchange of Se with sulfite at the CdSO_3 surface to give a disordered CdSe , which breaks off from the large crystal and crystallizes (or vice versa, we cannot tell which occurs first, or even if they occur in parallel). The fact that the CdSe separates from the CdSO_3 rather than forming a core-shell structure suggests a relatively large lattice mismatch between the two compounds along some of the growth planes (some of the lattice spacing is similar between the two compounds, others different).

XRD of the yellow precipitate is extremely broad and irregular, extending from a 2θ of ca. 20° to ca. 40° . Sometimes we see peaks corresponding to certain reflections of CdSO_3 ; often we see none. This broad pattern is not due to CdSe but almost certainly to a convolution of broader peaks of CdSO_3 , which exhibits many different peaks in this region: the large crystals of CdSO_3 (sharp peaks) have already largely broken down to small crystals (giving the broad envelope), as seen also in the TEM study.

We can compare this reaction to the reaction of selenosulfate with basic lead carbonate or with hydrated lead oxide ("lead hydroxide"), where the large crystals of lead carbonate and of hydrated oxide break down in the process of forming PbSe .⁶

Both EDS and ICP analyses of the "final" (after 90 min of reaction) orange precipitate show that the S/Se ratios are now reversed with ca. 3 times as much Se as S and only several percent excess Cd. A large part of the CdSO_3 has been converted to CdSe as well as any $\text{Cd}(\text{OH})_2$ which may have been present. We note that the analyzed precipitates were rinsed with ethanol. Rinsing in Na_2SO_3 solution, which can dissolve CdSO_3 by complexing it into a polysulfite ion, resulted in a reduction of the S content of the precipitate (by ca. 50%

(6) Gorer, S.; Albu-Yaron, A.; Hodes, G. *Chem. Mater.* **1995**, 7, 1243.

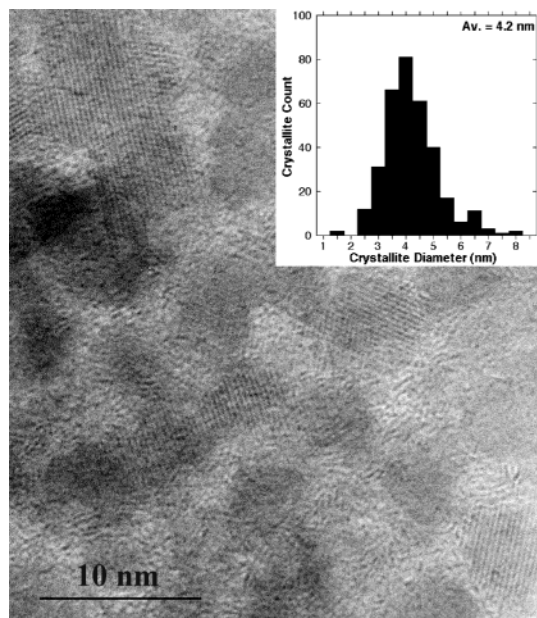


Figure 4. High-resolution TEM micrograph of the orange precipitate. Inset: Size distribution of the crystals in this precipitate.

for the yellow precipitate and ca. 40% for the orange one).

TEM imaging of this orange precipitate (Figure 4) showed a variation of crystal sizes with most between 3 and 5 nm and with an average size of 4.2 nm. (Another TEM analysis of a different, but similarly prepared, sample gave an average size of 4.4). While we carried out lattice imaging of these samples, CdSO₃ has many spacings, some of which essentially overlap with those of CdSe, and while we can often assign a crystal to CdSO₃, we cannot reliably state that a particular crystal is, indeed, CdSe. However, from the EDS analysis, we can infer that ca. 75% of the material is CdSe and will not be far out if we assume that the average size calculated from the size distribution reflects that of the CdSe.

In contrast to the yellow precipitate, XRD gives peaks for the orange precipitate which can be correlated with sphalerite CdSe (Figure 5). We sometimes see slight structure in the main peak at ca. 25° which can be attributed to a small concentration of wurtzite CdSe (which was seen also in the ED measurements). For this reason, we use the peak at ca. 42° for measuring the coherence length, and since this peak is also somewhat (although less) distorted on the high-angle side by a nearby reflection, we use only the low-angle half of the peak and assume it is symmetrical. This gives a coherence length of 3.8 nm (several XRD spectra were taken of different samples, giving a variation in estimated size from 3.5 to 4.2 nm). We can compare this with the value of 4.2 nm measured by TEM imaging.

While we have followed the development of the formation of CdSe, we are unable to specify the pathway of CdSe formation. The two main possibilities normally considered (usually based on the presence of a solid hydroxide phase—in the present study, we have an initial solid sulfite phase) are formation of free selenide ion, which reacts with the CdSO₃, or formation of a complex compound between the selenosulfate and the CdSO₃, which then dissociates to give CdSe. As men-

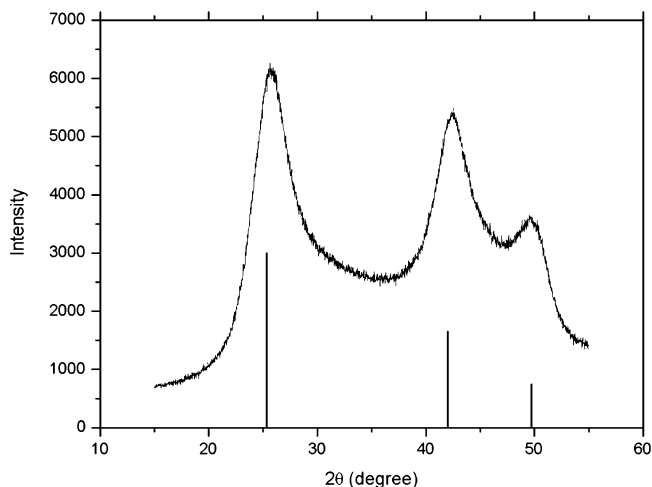


Figure 5. XRD spectrum of orange precipitate (after 90 min of reaction). The PDF data for sphalerite CdSe are given as vertical lines.

tioned previously, it is difficult to distinguish between these two possibilities. However, both chemical considerations of the reaction as well as observations made by us during this study suggest the possibility of a further route, as follows.

The selenosulfate solution is actually in equilibrium with sulfite and elemental Se:

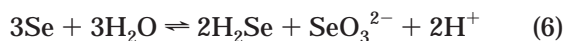


Se will precipitate out from this solution if the SO₃²⁻ concentration falls sufficiently. This will occur when CdSO₃ precipitates at the beginning of the presently investigated reaction. It will also occur if the pH is low (less than ca. 7), through the pH-dependent equilibrium between SO₃²⁻, HSO₃⁻, and SO₂. We do not observe visually the formation of any immediate coloration (precipitated Se is normally orange-red), which would suggest that this occurs. However, if a selenosulfate solution is acidified (pH ca. 3.5) forming Se, and Cd²⁺ is subsequently added, there is a slow change (over some days) in color of the Se from red to orange with eventual formation of CdSe. It is possible that this reaction occurs by reaction of Cd²⁺ (CdSO₃ does not visibly precipitate at this pH) with a very low concentration of selenosulfate present in the low pH solution. If this is so, then the reaction is similar to the one at higher pH but without the presence of the solid CdSO₃ phase—that is, it is a homogeneous reaction in solution. However, a very rough (some parameters can only be roughly estimated) thermodynamic calculation based on the equilibrium constant of hydrolysis of selenosulfate (1.6×10^{-31})⁷ implies that the concentration of Se²⁻ formed would be too low to form CdSe. {This calculation is based on the equilibrium constant K_s for hydrolytic decomposition of selenosulfate as given in ref 7, where $K_s = ([\text{Se}^{2-}][\text{H}^+]^2[\text{SO}_4^{2-}]) / (K_{\text{H}_2\text{Se}}[\text{SeSO}_3^{2-}])$. [Se²⁻] can then be calculated from the concentrations of reactants used, a value of 1.3×10^{-15} for $K_{\text{H}_2\text{Se}}$ and assuming some reasonable value for [SO₄²⁻], which is a product of the decomposition of selenosulfate (and will probably also be present in small amounts from oxidation of sulfite),

(7) Kitaev, G. A.; Khvorenkova, A. Zh. *Russ. J. Appl. Chem.* **1998**, *71*, 1325.

of 0.001 M. This gives a value for $[\text{Se}^{2-}]$ of 2×10^{-37} . Since the solubility product of CdSe is ca. 4×10^{-35} , we would need ca. 10^{-32} M Se^{2-} to allow formation of CdSe—5 orders of magnitude less than the estimated quantity.}

There are other possible pathways for reaction between solid Se in water and Cd^{2+} . Se can very slightly dissolve in water through a disproportionation reaction to form selenide:



While the concentration of selenide will be extremely low, because of the very low solubility product of CdSe (of the order of 10^{-35}) together with the high concentration of Cd^{2+} , very little selenide is needed to precipitate CdSe and remove the H_2Se , thereby maintaining the shift in equilibrium to the right. Another possibility is specific adsorption of Cd^{2+} ions at the solid Se surface as the first stage of CdSe formation. We will investigate this reaction for CdSe formation more fully.

We can correlate the measured or estimated crystal sizes of the various CdSe samples with measured band gaps estimated from the optical transmission spectra. From Figure 1, we can estimate band gaps from the transmission spectra of ca. 2.55 eV for the yellow precipitate 5 min after the start of the reaction and ca. 2.25 eV for the final orange state. Using earlier measurements we have made on chemically deposited CdSe films, 2.25 eV corresponds to a crystal size of ca. 3.7 nm.⁸ We note that our correlation between crystal size and band gap gives values of band gaps ca. 0.06–0.08 eV (the latter value for crystals <4 nm) higher than those reported by Murray et al. for wurtzite CdSe.⁹ The

minimum band gap we obtain with chemically deposited films of sphalerite CdSe for clearly nonquantized crystals (12–20 nm in size) is 1.8 eV, in agreement with the value given in Landolt-Börnstein for sphalerite CdSe.¹⁰

Because of the wide size and shape distribution of the yellow precipitate and our lack of knowledge of which crystals correspond to CdSe and not CdSO_3 , any correlation of the band gap of this precipitate will be crude. While we cannot make films with a band gap as high as 2.6 eV, using the data of Rogach¹¹ (whose XRD data could be interpreted as sphalerite or hexagonal with stacking faults), 2.55 eV is equivalent to a crystal size of ca. 2.5 nm. While the average size of the crystals in the yellow precipitate (3.1 nm) is larger than this, there are many crystals in this distribution around this size.

In conclusion, we have investigated the formation of CdSe nanocrystals from selenosulfate solutions, showing how the initially formed CdSO_3 is converted into CdSe. Rather than form a core-shell structure in which Se gradually substitutes for SO_3 , the CdSe forms a thin shell of disordered material around the CdSO_3 , and then breaks off the parent CdSO_3 to form isolated nanocrystals, probably due to mismatch strain at the CdSe/ CdSO_3 interface. Different pathways than usually considered for the formation of CdSe from selenosulfate have been suggested as possible under certain reaction conditions. The spectral changes of the precipitate formed during the reaction correlated with the band gaps predicted by size quantization.

Acknowledgment. We thank Dr. Ronit Popovitz-Biro for help with the electron microscopy measurements. This research was supported by the Israel Science Foundation, Jerusalem, Israel.

CM049895V

(8) Sarkar, S.; Chandrasekharan, N.; Gorer, S.; Hodes, G. *Appl. Phys. Lett.* **2002**, *81*, 5045.

(9) Murray, C. B.; Norris, D. J.; Bawendi, M. G. *J. Am. Chem. Soc.* **1993**, *115*, 8706.

(10) Landolt-Börnstein, Eds. Madelung, O.; Schulz, M.; Weiss, H., Springer-Verlag: New York, 1982; Vol. 17b.

(11) Rogach, A. L.; Kornowski, A.; Gao, M. Y.; Eychmüller, A.; Weller, H. *J. Phys. Chem. B* **1999**, *103*, 3065.